PROCEEDINGS OF SCIENCE

Interpreting the IceCube events by decaying dark matter

Arman Esmaili[*a] **and Pasquale D. Serpico**[b]

[a] *Departamento de Física, Pontifícia Universidade Católica do Rio de Janeiro, C. P. 38071, 22452-970, Rio de Janeiro, Brazil*

[b] *LAPTh, Univ. de Savoie Mont Blanc, CNRS, B.P.110, Annecy-le-Vieux F-74941, France*

E-mail: arman@puc-rio.br, serpico@lapth.cnrs.fr

We review the interpretation of observed neutrino flux at IceCube experiment in terms of PeV-scale decaying dark matter. We report on the energy and angular distributions expected from decaying dark matter and confront it with the IceCube data. By performing various statistical tests we conclude that currently the data show a mild preference for the decaying dark matter scenario from both angular and energy distribution analyses. We discuss the prospects of probing this scenario by extensive air shower (EAS) cosmic ray experiments. We show that the current EAS experiments can probe a part of the parameter space of this scenario, through observation of gamma-ray flux or anisotropy measurement, and forthcoming EAS experiments can improve the limit significantly.

The 11th International Workshop Dark Side of the Universe 2015
14-18 December 2015
Kyoto, Japan

*Speaker.

PoS(DSU2015)047

1. Introduction

The IceCube experiment observed a flux of high energy neutrinos in the range of 10 TeV - 2 PeV, by analyzing the starting events in the detector and using a part of the detector as veto to reject background events from atmospheric muons and neutrinos (the so-called HESE analysis) [1, 2, 3]. An immediate quest after this observation is the identification of possible sources that can contribute to this flux of neutrinos. Several astrophysical sources have been proposed and various multi-messenger studies are under consideration in the search for such correlations (in fact some class of the sources are already in tension; *e.g.*, see [4, 5] for the case of star-forming galaxies). On the other hand, comparing the energy scale of the IceCube neutrinos with the previously observed neutrino fluxes points to the fact that the recent neutrinos are orders of magnitude higher in energy and so it will not be surprising to see signatures of new physics in them, especially since in the high energy range neutrinos are the only messenger propagating in the Universe almost intact. In this regards, we will discuss the possibility to interpret the IceCube neutrino flux in terms of PeV-scale mass decaying dark matter [6, 7]. We will elaborate on the expected signatures in this scenario, mainly the energy and angular distributions of the resulting neutrino flux and confront them with the reported data by IceCube collaboration. Also, we will explore possible ways of excluding/verifying this scenario, especially through the EAS experiments [8].

2. Energy distribution

The neutrino flux from dark matter decay consists of two contributions: Galactic and extra-galactic components. While in the case of annihilating dark matter the latter is often subleading and dependent on the poorly known small scale clustering properties, for decaying dark matter the contributions of both fluxes are comparable and their relative contribution is robustly known. The Galactic component of neutrino flux originates from the decay of dark matter particles in our galaxy's halo with the differential flux (see [9, 10]):

$$\frac{\mathrm{d}J_{\mathrm{h}}}{\mathrm{d}E_\nu}(l,b) = \frac{1}{4\pi\, m_{\mathrm{DM}}\, \tau_{\mathrm{DM}}} \frac{\mathrm{d}N_\nu}{\mathrm{d}E_\nu} \int_0^\infty \mathrm{d}s\; \rho_{\mathrm{h}}\left[r(s,l,b)\right] , \tag{2.1}$$

where (l,b) are the Galactic coordinates, m_{DM} and τ_{DM} are the dark matter mass and lifetime, respectively, and $\rho_{\mathrm{h}}(r)$ is the density profile of DM particles in our Galaxy as a function of distance from the Galactic center, r. Here we take the NFW profile for ρ_{h}. The dN_ν/dE_ν is the energy spectrum of neutrinos produced in the decay of a dark matter particle. The line-of-sight integration parameter s is related to r by $r(s,l,b) = \sqrt{s^2 + R_\odot^2 - 2sR_\odot \cos b \cos l}$, where $R_\odot \simeq 8.5\,\mathrm{kpc}$ is the Sun to Galactic center distance.

The extragalactic component of the neutrino flux, originating from the dark matter decay at cosmological distances (and hence isotropic to the leading order and independent of the Galactic coordinates) has the differential flux

$$\frac{\mathrm{d}J_{\mathrm{eg}}}{\mathrm{d}E_\nu} = \frac{\Omega_{\mathrm{DM}}\rho_{\mathrm{c}}}{4\pi m_{\mathrm{DM}}\tau_{\mathrm{DM}}} \int_0^\infty \mathrm{d}z\, \frac{1}{H(z)} \frac{\mathrm{d}N_\nu}{\mathrm{d}E_\nu}\left[(1+z)E_\nu\right], \tag{2.2}$$

where $H(z) = H_0\sqrt{\Omega_\Lambda + \Omega_{\mathrm{m}}(1+z)^3}$ is the Hubble expansion rate as a function of redshift z and $\rho_{\mathrm{c}} = 5.5\times10^{-6}\,\mathrm{GeV\,cm^{-3}}$ is the critical density of the Universe. For the cosmological parameters

we take the values derived from the Planck temperature map data. Integration over the solid angle of Eqs. (2.1) and (2.2) gives the energy spectrum of neutrinos.

The total spectrum of neutrinos (that is galactic + extragalactic) strongly depends on the dN_ν/dE_ν which in turn depends on the particle physics model which can accommodate PeV-scale decaying dark matter. A general phenomenological description of the spectrum (decomposable to *soft* and *hard* channels) is given in [6]. From theoretical point of view, a portal Lagrangian of the form $\mathscr{L}_{\rm portal} = \mathscr{O}_{\rm SM}\mathscr{O}_{\rm DM}/\Lambda^{d-4}$, where $\mathscr{O}_{\rm SM}$ and $\mathscr{O}_{\rm DM}$ are gauge-invariant operators composed solely of the standard model and dark sector fields, respectively, d is the dimension of the portal operators, and Λ is an energy scale. The assignment $\mathscr{O}_{\rm SM} = H\,L$ defines the *neutrino portal* models, where H and L are the Higgs and lepton doublets. The lowest dimensional Lagrangian can be constructed by taking $\mathscr{O}_{\rm DM}$ equal to a spin-1/2 gauge singlet neutrino N identified with the dark matter candidate. The details of this mode is given in [11]. The main feature of this model is that all the decay channels of dark matter particle and their branching ratios can be calculated: at tree level, the dark matter particle decays to $\ell^\pm W^\mp$, $\nu_\ell Z$ and $\nu_\ell h$ channels with the relative branching ratios $2:1:1$. Even the flavor structure of decay channels can be determined: the $\mathrm{Br}(\ell^\pm W^\mp) = |U_{\ell 1}|^2$ ($|U_{\ell 3}|^2$) for normal (inverted) hierarchy of neutrino masses. Figure 1 shows the energy distribution of events for a 4 PeV dark matter mass, including both the dark matter signal and the atmospheric residual background (only relevant at low energies), for the NH model (left panel) and IH model (right panel). The width of the shaded regions corresponds to variation of dark matter lifetime $\tau_{\rm DM}$ within 1σ range around the best-fit point obtained from the fit to IceCube data ($\tau_{\rm DM} = 7.3\times10^{27}$ s for NH and $\tau_{\rm DM} = 1.1\times10^{28}$ s for IH). The dashed green line shows the expected events for an $E_\nu^{?2}$ astrophysical spectrum. Qualitatively, this dark matter model (which is the simplest one!) is in a better agreement with the data than the astrophysical one above about 300 TeV, and in slightly worse agreement at lower energies.

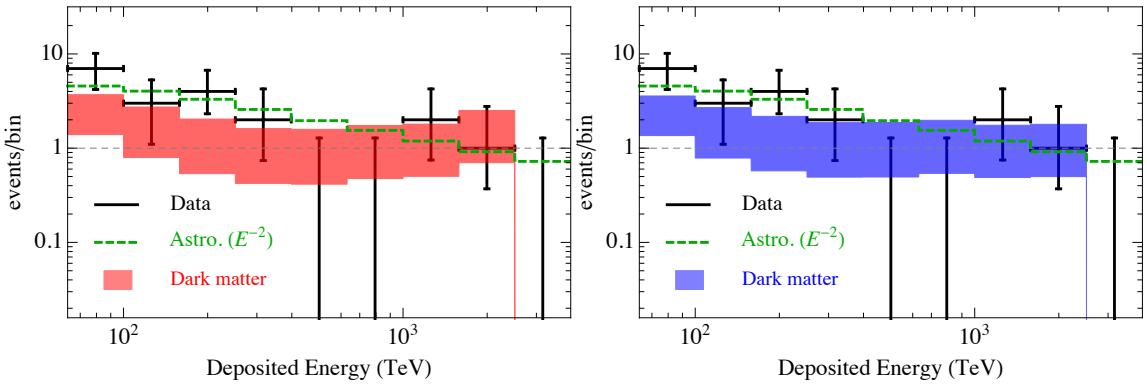

Figure 1: The energy distribution of events in DDM scenario

Higher dimensional portal Lagrangians can be constructed: for example by assigning $\mathscr{O}_{\rm DM} = \chi\phi$, where χ is a singlet fermion and ϕ a singlet scalar, dimension 5 portal Lagrangian can be obtained. Clearly higher dimensional and more sophisticated models can be constructed. However, qualitatively, in the higher-dimensional operator models there is more freedom in choosing the relative branching ratios among the *soft* and *hard* channels, as they are not fixed within the model. As can be seen from the Figure 1 already with the most constrained model, corresponding to the

dimension-4 operator, an acceptable fit to the IceCube data can be obtained and so obviously the same or better fits can be obtained in higher dimensional portals.

3. Angular distribution

The energy integration of Eqs. (2.1) and (2.2) gives the angular distribution of neutrinos from dark matter decay. The angular probability distribution function (PDF) from decaying dark matter is given by

$$p^{\rm DM}(b,l) = \kappa \left(\int_0^\infty {\rm d}s \; \rho_{\rm h}[r(s,l,b)] + \Omega_{\rm DM}\rho_c\beta \right) , \tag{3.1}$$

where $\beta = \int_0^\infty {\rm d}z/[(1+z)H(z)]$ and $\kappa = 1/[4\pi\,(\eta + \Omega_{\rm DM}\rho_c\beta)]$, where η is a constant that can be derived from normalization condition. It is worth to emphasize that in the case of decaying dark matter, the relative contribution of Galactic (which is centered at Galactic center) and extragalactic (which is isotropic) components is fixed; the total PDF has a mild concentration around the Galactic center and flattens out to quasi-isotropic when moving to larger latitudes and longitudes. For the case of isotropic distribution (which is the case for astrophysical neutrinos), obviously the PDF is $p^{\rm iso}(b,l) = 1/4\pi$.

In our angular distribution analysis we will answer to the following question: whether the angular distribution of data prefer a DM-like distribution or isotropic one? and what is the significance of preference? various statistical methods can be used in answering this question. A detailed analysis can be found in [7]. Here we briefly summarize the result of a likelihood analysis and Anderson-Darling test.

Likelihood analysis: For each event we can define a probability distribution function p_i. In the "flat sky" approximation

$$p_i(b,l) = \frac{1}{2\pi\sigma_i^2} \exp\left[-\frac{|\vec{x}_i - \vec{x}|^2}{2\sigma_i^2} \right] , \tag{3.2}$$

where $|\vec{x}_i - \vec{x}|$ is the angular distance between two points and σ_i is the error in the reconstruction of direction reported by IceCube. We analyze the 35 events collected during three years at IceCube detector [3]. The following test statistics (TS) can be defined for the likelihood analysis:

$${\rm TS}_{\rm like} = 2\sum_{i=1}^{N} \left(\ln f_i - \ln p_i^{\rm iso} \right) = 2\ln\left(\prod_{i=1}^{N} f_i \right) - 2N\ln\left(\frac{1}{4\pi} \right) , \tag{3.3}$$

where

$$f_i = \int p_i(b,l)\; p^{\rm DM}(b,l)\cos(b)\;{\rm d}b\;{\rm d}l = \frac{1}{2\pi\sigma_i^2} \int e^{-\frac{|\vec{x}_i-\vec{x}|^2}{2\sigma_i^2}}\; p^{\rm DM}(b,l)\cos(b)\;{\rm d}b\;{\rm d}l \; . \tag{3.4}$$

In the formulae above, N refers to the number of signal events. It would be by far too optimistic to assume that $N = 35$ events, since according to IceCube, a number of background events given by $N_b = 15^{+10.1}_{-5.8}$ contaminates the sample. For illustrative purposes, let us assume that $N_b = 15$, namely the reported central value by IceCube, which means that $N = 20$ in eq. (3.3). However, still we do not know *which* events are background and which ones are signal. To simplify a bit the combinatorics problem, we can nonetheless make the assumption that none of the events with

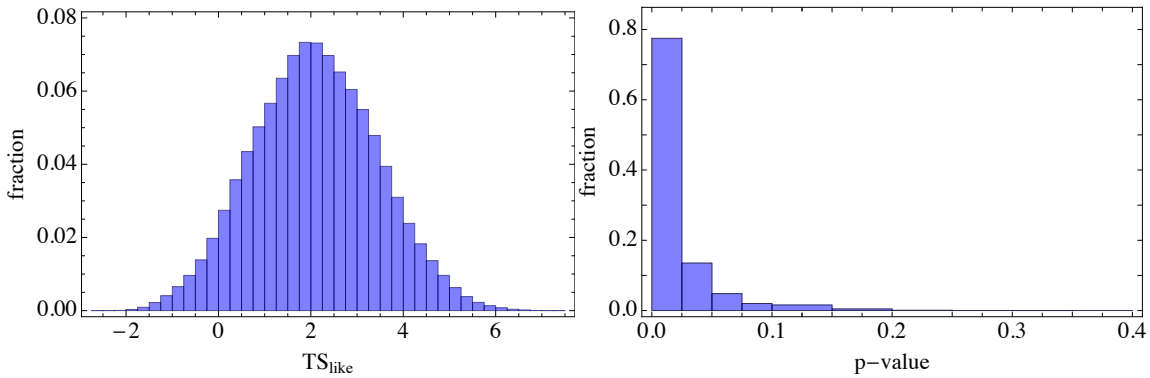

Figure 2: Left panel: histogram of the fraction of realizations out of $\binom{26}{15}$ having $\mathrm{TS}_{\mathrm{like}}$ value within the shown bins. Right panel: histogram of the fraction of realizations out of $\binom{26}{15}$ having p-values in the shown bins.

energy $E_\nu > 150$ TeV is due to background (that is atmospheric neutrinos or muons) since IceCube collaboration estimates the number of background events in that range of energy $\ll 1$. This leaves $\binom{26}{15} = 7,726,160$ ways of selecting which events are background, among the low energy events. For each case we calculate the $\mathrm{TS}_{\mathrm{like}}$ value, whose distribution (with the mean value $\overline{\mathrm{TS}}_{\mathrm{like}} = 2.1$) is shown in left panel of Figure 2. To estimate the p-value, we generated a similar distribution of $\mathrm{TS}_{\mathrm{like}}$ values from $\sim 10^5$ sets of isotropically distributed 20 events datasets. For each realization of $\binom{26}{15}$ set, we calculate the p-value by comparing its $\mathrm{TS}_{\mathrm{like}}$ with the $\mathrm{TS}_{\mathrm{like}}$ values of generated events (simply, the p-value is the fraction of generated events which have smaller $\mathrm{TS}_{\mathrm{like}}$ values than the one computed by observed data). The right panel of Figure 2 shows the distribution of computed p-values. It is clear graphically that data prefer mildly the DM angular distribution rather than isotropic distribution. The average p-value is found to be $\sim 2\%$, which means a $\sim 98\%$ C.L. preference for DM distribution.

Anderson-Darling test: An alternative statistical test, the AD test, can be performed to quantify the compatibility of data with DM vs. isotropic distributions. The AD test is a powerful test with several advantages, such as its *non-parametric* nature and sensitivity to difference in end-points of tested PDFs. By taking into account the symmetry, the problem can be reduced to one dimension: the DM distribution only depends on the angle ϑ measuring the angular distance from Galactic center and not on the azimuthal angle φ. This allows one to use ϑ as the only variable, suitable for a one-parameter test. The 1-dimensional isotropic and DM distribution functions are: $p^{\mathrm{iso}}(\vartheta) = \int_0^{2\pi} p^{\mathrm{iso}}(\vartheta,\varphi)\,\mathrm{d}\varphi = 1/2$ and $p^{\mathrm{DM}}(\vartheta) = \int_0^{2\pi} p^{\mathrm{DM}}(\vartheta,\varphi)\,\mathrm{d}\varphi$. The AD test compares the *empirical distribution function* (EDF) of data with the cumulative distribution function (CDF) of the distribution being tested. The EDF of data is given by

$$\mathrm{EDF}^{\mathrm{data}}(\vartheta) = \frac{1}{N}\sum_{i=1}^{N}\Theta(\vartheta - \vartheta_i) \tag{3.5}$$

where N is the number of signal events and Θ is the Heaviside step function. The CDF of DM and

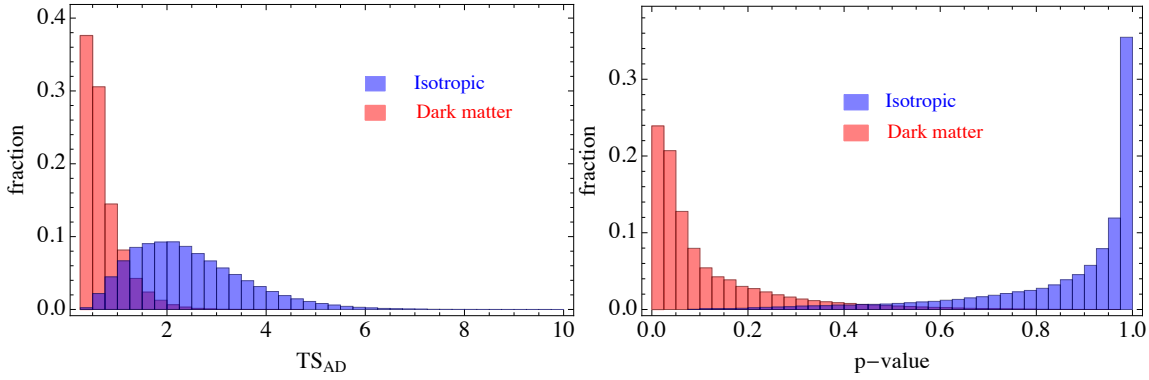

Figure 3: Same as Figure 2 for AD test. In both panels the red (blue) color corresponds to comparison of EDF of data with DM (isotropic) CDF.

isotropic distributions can be calculated as:

$$\mathrm{CDF}^{\mathrm{DM}}(\vartheta) = \int_0^{\vartheta} p^{\mathrm{DM}}(\vartheta')\sin\vartheta' d\vartheta' \,, \tag{3.6}$$

and,

$$\mathrm{CDF}^{\mathrm{iso}}(\vartheta) = \int_0^{\vartheta} p^{\mathrm{iso}}(\vartheta')\sin\vartheta' d\vartheta' = \frac{1-\cos\vartheta}{2} \,. \tag{3.7}$$

The AD test statistics estimator is defined as

$$\mathrm{TS}_{\mathrm{AD}} = -N - \frac{1}{N}\sum_{i=1}^{N}(2i-1)\left[\ln\left(\mathrm{CDF}^{\mathrm{DM}}(\vartheta_i)\right) + \ln\left(1-\mathrm{CDF}^{\mathrm{DM}}(\vartheta_{N+1-i})\right)\right] \,, \tag{3.8}$$

and similarly for the isotropic distribution. Here again $N = 20$. Like the likelihood test, we calculate the $\mathrm{TS}_{\mathrm{AD}}$ for all the possible ways of dropping the 15 background events from the 35 events. Left panel of Figure 3 shows the distribution of $\mathrm{TS}_{\mathrm{AD}}$ for all the possible realization, for both DM and isotropic distributions, which the statistically larger $\mathrm{TS}_{\mathrm{AD}}$ for isotropic distribution indicates the preference of data for DM distribution. To calculate the p-value, we generate $\sim 10^5$ sets of events (each including 20 events) according to the isotropic distribution and for each set we calculate the $\mathrm{TS}_{\mathrm{AD}}$ for both DM and isotropic distributions. As in the likelihood test, for each realization of background choosing (that is $\binom{26}{15}$ ways) the p-value is calculated by comparing the $\mathrm{TS}_{\mathrm{AD}}$ of that realization with the $\mathrm{TS}_{\mathrm{AD}}$ distribution of generated events, that is the fraction of generated events having smaller $\mathrm{TS}_{\mathrm{AD}}$. Right panel of Figure 3 shows the distribution of p-values for all the realizations of $\binom{26}{15}$ ways. The separation of the DM and isotropic distributions under the AD test is obvious, with clearly smaller values of the estimator for the DM case with respect to isotropic one. This confirms the results of likelihood analysis. Quantitatively, 11% of generated isotropic sample have smaller $\mathrm{TS}_{\mathrm{AD}}$ than the values obtained for data vs. DM distribution (for comparison, 86% of generated isotropic sample have smaller $\mathrm{TS}_{\mathrm{AD}}$ than the values obtained for data vs. isotropic distribution.)

4. Prospects of testing DDM in EAS experiments

The DDM interpretation of IceCube events can be tested by looking for the expected accompanying gamma-ray flux. The Universe is opaque to gamma-rays with energy $\sim$ PeV and so the only

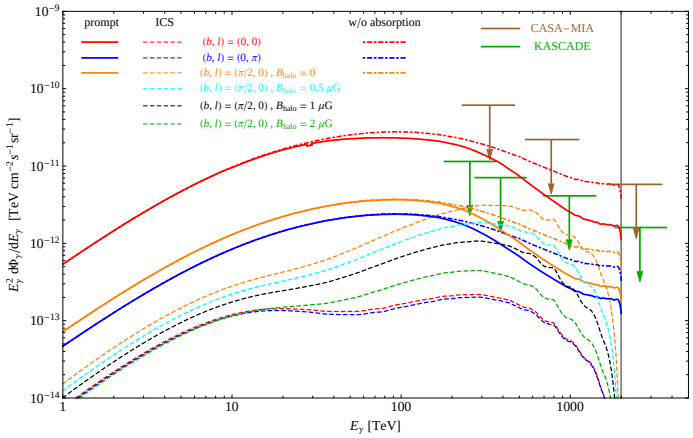

Figure 4: The expected gamma-ray flux in DDM scenario.

component of gamma-ray flux that can reach the Earth (without significant alteration) is the Galactic component[1]. However, even the Galactic sky is partially opaque to $\sim$ PeV gamma-ray and the effect of absorption should be taken into account. The Galactic gamma-ray flux from DDM consists of prompt and inverse Compton produced fluxes. A detailed calculation of these fluxes is given in [8]. The result is summarized in figure 4, assuming $m_{\rm DM} = 4\,$PeV and $\tau_{\rm DM} = 10^{28}\,$s in NH model. The solid curves depict the prompt flux, from GC (red, top), anti-GC (blue, bottom) and Galactic Pole (orange, intermediate). In each of these curves the dot-dashed curve deviating from the solid curve at higher energies shows the flux neglecting the absorption of γ-rays. When comparing the expected γ-ray flux from DDM with the experimental bounds, the importance of accounting properly for the absorption of γ-ray on CMB photons is manifest, particularly at high energy. The dashed curves in figure 4 show the IC flux: the red (blue) dashed curves are the IC flux form GC (anti-GC) direction. The orange dashed curve shows the IC flux from the Galactic pole direction, with the assumption that the Galactic magnetic field only consists of the (thin disk) regular field; i.e., $B_{\rm halo} = 0$. The cyan, black and green dashed curves show the IC flux from the Galactic pole within the assumptions $B_{\rm halo} = 0.5$, 1 and 2 μG, respectively. Finally, the green and brown bar lines with arrows show, respectively, the upper limits on the γ-ray flux inferred by CASA-MIA and KASCADE experiments.

Despite the fact that current EAS bounds are not yet constraining enough for the DDM explanations of IceCube events, the interesting parameter space appears within reach. Also, *anisotropy studies alone*, even without shower property discrimination capabilities, might contribute to the constraints. EAS experiments in fact routinely measure cosmic ray anisotropy, albeit often only in terms of some "partial estimator" like the dipolar anisotropy (averaged with respect to right ascension). The prompt flux from DDM can contribute to this anisotropy. An immediate constraint on DM lifetime can be obtained by requiring that anisotropy induced by gamma-rays should not exceed the observed total anisotropy in cosmic rays. In practice, by requiring that in no energy bin

[1]The extragalactic high energy gamma-rays develop a cascade by successive pair production - inverse Compton scattering on extragalactic background light and CMB. The cascades gamma-rays fall in the energy range $100 - 1000$ GeV and contribute to the IGRB detected by Fermi-LAT. The DDM scenario is compatible with the IGRB data [12].

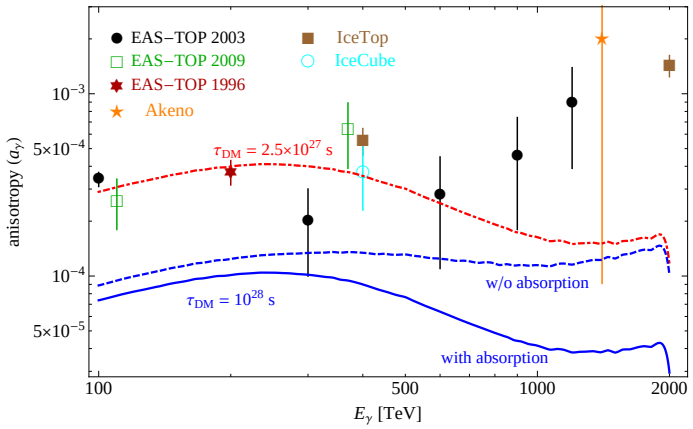

Figure 5: Anisotropy

anisotropy exceeds by more than two sigma of the measured value, we can obtain a conservative bound on the DM lifetime as $\tau_{\rm DM} > 2.5 \times 10^{27}$ s. The power of this observable is due to the fact that the intrinsic anisotropy in charged cosmic rays is at the level of $10^{-4} \div 10^{-3}$, while a much larger (by two to three orders of magnitude!) relative anisotropy in gamma-rays is expected, at very least due to the off-center position of the Sun in the Galaxy. This means that, despite the fact that gamma-rays only constitute a small fraction of the overall CR flux at $0.1 - 1$ PeV energies, in the anisotropy observable one can benefit from a larger signal to noise ratio. Accounting for absorption, however, suppresses the gamma-ray anisotropy, since pair-production is more severe in the GC direction than the anti-GC direction. In figure 5 the blue solid (dashed) curve shows the expected anisotropy (without) taking into account the absorption, for the fiducial choice of lifetime discussed previously; while the red dot-dashed curve corresponds to the limiting value when it exceeds the measured anisotropy at 2σ. For comparison, we also report the amplitudes of dipolar anisotropies measured by different experiments.

References

[1] M. G. Aartsen *et al.* [IceCube Collaboration], Phys. Rev. Lett. **111**, 021103 (2013) [arXiv:1304.5356 [astro-ph.HE]].

[2] M. G. Aartsen *et al.* [IceCube Collaboration], Science **342**, 1242856 (2013) [arXiv:1311.5238 [astro-ph.HE]].

[3] M. G. Aartsen *et al.* [IceCube Collaboration], Phys. Rev. Lett. **113**, 101101 (2014) [arXiv:1405.5303 [astro-ph.HE]].

[4] K. Emig, C. Lunardini and R. Windhorst, JCAP **1512**, 029 (2015) [arXiv:1507.05711 [astro-ph.HE]].

[5] K. Bechtol, M. Ahlers, M. Di Mauro, M. Ajello and J. Vandenbroucke, arXiv:1511.00688 [astro-ph.HE].

[6] A. Esmaili and P. D. Serpico, JCAP **1311**, 054 (2013) [arXiv:1308.1105 [hep-ph]].

[7] A. Esmaili, S. K. Kang and P. D. Serpico, JCAP **1412**, no. 12, 054 (2014) [arXiv:1410.5979 [hep-ph]].

[8] A. Esmaili and P. D. Serpico, JCAP **1510**, no. 10, 014 (2015) [arXiv:1505.06486 [hep-ph]].

[9] A. Esmaili, A. Ibarra and O. L. G. Peres, JCAP **1211**, 034 (2012) doi:10.1088/1475-7516/2012/11/034 [arXiv:1205.5281 [hep-ph]].

[10] A. Ibarra, D. Tran and C. Weniger, Int. J. Mod. Phys. A **28**, 1330040 (2013) doi:10.1142/S0217751X13300408 [arXiv:1307.6434 [hep-ph]].

[11] T. Higaki, R. Kitano and R. Sato, JHEP **1407**, 044 (2014) [arXiv:1405.0013 [hep-ph]].

[12] K. Murase, R. Laha, S. Ando and M. Ahlers, Phys. Rev. Lett. **115**, 071301 (2015) [arXiv:1503.04663 [hep-ph]].